

Article

# Numerical and Computational Analysis of a New Vertical Axis Wind Turbine, Named KIONAS

Eleni Douvi <sup>1,\*</sup>, Dimitra Douvi <sup>1,\*</sup>, Dionissios Margaris <sup>1,\*</sup> and Ioannis Drosis <sup>2</sup>

<sup>1</sup> Fluid Mechanics Laboratory (FML), Mechanical Engineering and Aeronautics Department, University of Patras, GR-26500 Patras, Greece

<sup>2</sup> Small Wind Turbines Development Manager, 97 Dimitros Street, GR-19200 Elefsina, Greece; giannisdrosis@hotmail.com

\* Correspondence: douvi@mech.upatras.gr (E.D.); dimdouvi@gmail.com (D.D.); margaris@mech.upatras.gr (D.M.)

Academic Editor: Demos T. Tsahalis

Received: 12 December 2016; Accepted: 5 January 2017; Published: 11 January 2017

**Abstract:** This paper concentrates on a new configuration for a wind turbine, named KIONAS. The main purpose is to determine the performance and aerodynamic behavior of KIONAS, which is a vertical axis wind turbine with a stator over the rotor and a special feature in that it can consist of several stages. Notably, the stator is shaped in such a way that it increases the velocity of the air impacting the rotor blades. Moreover, each stage's performance can be increased with the increase of the total number of stages. The effects of wind velocity, the various numbers of inclined rotor blades, the rotor diameter, the stator's shape and the number of stages on the performance of KIONAS were studied. A FORTRAN code was developed in order to predict the power in several cases by solving the equations of continuity and momentum. Subsequently, further knowledge on the flow field was obtained by using a commercial Computational Fluid Dynamics code. Based on the results, it can be concluded that higher wind velocities and a greater number of blades produce more power. Furthermore, higher performance was found for a stator with curved guide vanes and for a KIONAS configuration with more stages.

**Keywords:** vertical axis wind turbine; stator guide vanes; aerodynamic performance; power output; multi-stage

---

## 1. Introduction

Since the reserves of fossil fuels are diminishing, there is increasing interest in renewable energy sources, among which wind energy is included. Wind energy is harnessed by wind turbines, which can be either Horizontal Axis Wind Turbines (HAWT) or Vertical Axis Wind Turbines (VAWT). A considerable amount of literature has been published on HAWTs, because they are more effective than the VAWTs. Recently, there has been growing interest in VAWTs, because of their easy installation, manufacture and maintenance.

A review of various configurations of vertical axis wind turbines, along with their advantages and disadvantages, was first conducted by Aslam Bhutta et al. [1]. The techniques for VAWT design and the flow field over the blades were also reviewed. The results showed that the power coefficient is different for various configurations and can be optimized with tip speed ratio. The impact of structural parameters on the performance, particularly for Savonius wind turbine, is studied by Tang et al. [2]. Their findings revealed that for different structures, the maximum power coefficient can be increased by more than 30%.

Numerous investigations have been conducted to show the effects of guide vanes on vertical axis wind turbine performance. The first systematic study of the effects of guide vanes was reported by

Ejiri et al. [3], in 2006. A computational fluid dynamics (CFD) code was utilized to analyze the flow through the vertical axis cross-flow wind turbine and to propose an improved design configuration in order to achieve better performance, which had two guide vanes outside the turbine.

A year later, in 2007, Takao et al. [4] proposed a straight-bladed vertical axis wind turbine with a directed guide vane row, which was added to enhance its torque. The guide vane row improved the performance of the straight-bladed vertical axis turbine and the experimental results showed that the power coefficient of the proposed wind turbine was approximately 1.5 times higher than that of the original wind turbine which has no guide vane. A further study with more of a focus on the effect of guide vane geometry on the performance of wind turbine was conducted by the same researchers [5]. An experimental investigation was carried out, in order to investigate the effects of distance between the guide vanes and the number of guide vanes on power and torque coefficients. Recently, Shahizare et al. [6] simulated a vertical axis wind turbine with omni-direction guide vanes of eight different shape ratios to determine the effects of guide vanes. It was concluded that all the shape ratios improved the power and torque coefficient.

Kim and Gharib [7] studied the effect on the power output of the vertical axis wind turbine configuration by adding an upstream deflector. They found out that the dimensions and the relative position of the deflector are related to the power output of the VAWT. The optimal design of the wind booster, a device which controls the airflow around a vertical axis wind turbine, was also analyzed lately by Korprasertsak and Leephakpreeda [8]. This device consists of guide vanes mounted around the wind turbine, which not only accelerate but also direct the wind in order to impact the rotor blades at the most effective angle of attack. This results in an increase in the VAWT's angular speed and thus in power.

In order to improve a vertical axis wind turbine's performance, a stator is added around the rotor. The stator significantly increases the wind speed, and as a result it improves the self-starting behavior of the VAWT the power coefficient. The effect of a stator surrounding a vertical-axis wind turbine has been studied both experimental and numerical.

Simulations of a new power-augmented shroud integrated with a vertical axis wind turbine (VAWT) suitable for urban and suburban application were carried out by Wong et al. [9]. The results of the numerical simulation indicated that the new design for the power-augmented shroud is able to increase the coefficient of power significantly for the VAWT, by about 147.1% compared to the bare VAWT. At the same time, Nobile et al. [10] proposed and analyzed a computational investigation of an augmented wind turbine. The results of their study also showed that the introduction of an omnidirectional stator around the wind turbine increases not only the power but also the torque coefficients by around 30%–35% when compared to the open case. They also concluded that for optimum performance, attention needs to be given to the orientation of the stator blades.

Chen et al. [11,12] developed a vortical stator assembly (VSA) surrounding a vertical-axis wind turbine to improve rotor performance. The VSA consisted of six guide vanes, in order to guide the air tangentially into the VSA. The experimental results showed that the VSA significantly increased rotor performance and the rotor starting speed was reduced to approximately 1 m/s. The optimal VSA diameter was found to be approximately 1.82 times the rotor diameter.

The first systematic numerical and experimental study of the operating performance and power output from a vertical axis wind turbine was reported by Pope et al. [13]. They studied the effects of varying VAWT stator vane geometries of a Zephyr vertical axis wind turbine on the turbine's performance at constant and variable rotor velocities. Recently, Burlando et al. [14] have examined with a numerical wind turbine technique the effects of stator vanes on the flow around and inside a multi-stage vertical-axis wind turbine. They developed a numerical model to extend the results obtained by means of the physical model to more general conditions.

So far this type of vertical axis wind turbine has been applied to hybrid energy systems. Tong et al. [15] were the first to introduce a patented wind-solar hybrid renewable energy harvester for urban high rise application. The speed of the high-altitude free-stream wind is increased through

fixed or yaw-able power-augmentation-guide-vane (PAGV) before entering the wind turbine at the center portion. The geometry of the PAGV was optimized by computational fluid dynamics (CFD) simulation. The generated power was 1.25 times higher after integrating the PAGV with the VAWT. Chong et al. [16] introduced the Eco-Greenergy™ hybrid wind-solar photovoltaic energy generation system to power LED lights or other appliances. The system consists of a novel omni-direction guide vane with a vertical axis wind turbine and a PV panel mounted on the top surface. The system was found to generate a total of 572.8 kWh of energy per year, and the ODGV increases the annual wind energy output by 438%.

This project was undertaken to describe the design of a new vertical axis wind turbine, named KIONAS, and evaluate its performance using mathematical modelling and its aerodynamic behavior and flow field through Computational Fluid Dynamics (CFD) simulations.

The wind turbine examined in this study is a vertical axis wind turbine, which is named KIONAS. It consists of a rotor which is surrounded by a stator. In the rotors center there is a shaft, where a number of flat blades are mounted on, at an angle. The stator is added in order to increase the wind speed that impacts the rotor blades. The above system is a one-stage wind turbine KIONAS. The main characteristic of this wind turbine is that a multi-stage turbine can be constructed by adding more of the same stages to the first one, directly above it. The basic geometry of a three-stage wind turbine KIONAS is presented in Figure 1.

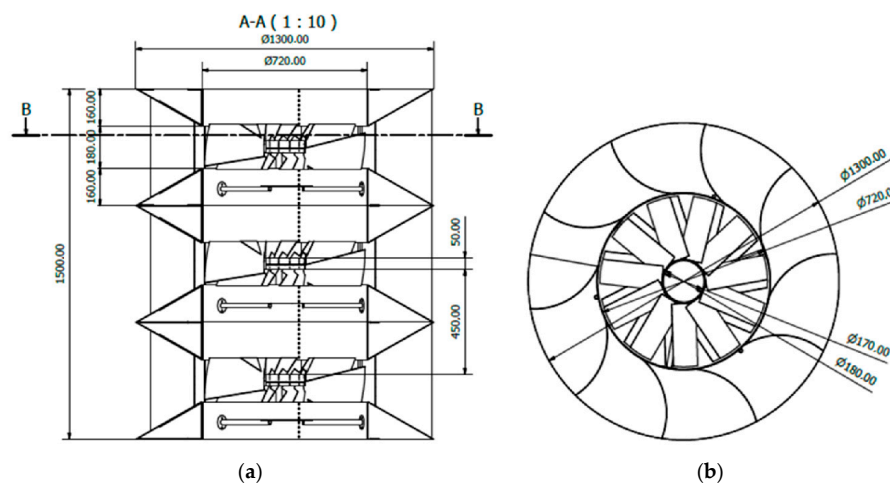


**Figure 1.** (a) The front view; (b) the top view of the basic geometry of a three-stage wind turbine KIONAS. Units in mm.

The current study contributes to our knowledge by drawing the following important conclusions. First of all, it was found that a multi-stage KIONAS could become advantageous in the long term because the output power per unit weight of the machine is higher as the number of KIONAS stages is increased and simultaneously the power of each individual stage is increased when an extra stage is added. Secondly, from the computational results it was obvious that part of the wind is directed both towards the upper and towards the lower stage for the two-stage KIONAS.

## 2. Numerical Computation

### 2.1. Mathematical Study

The first step in the mathematical study is the calculation of the resultant velocity of the air in each of the five sections of the front side of wind turbine KIONAS, Figure 2. The wind speed is considered equal to  $u_\infty$  and the average wind speed which enters each stator section,  $\bar{u}_{in}$ , is

$$\bar{u}_{in} = u_\infty \sin \varphi, \tag{1}$$

where  $\varphi = \frac{(2\nu-1)\pi}{10}$ , for  $\nu = 1, 2, 3, 4, 5$ . Thus, the average wind speed is:

$$\bar{u}_{in} = u_{\infty} \sin \frac{(2\nu - 1)\pi}{10} \tag{2}$$

The wind speed that impacts the rotor blades,  $\bar{u}$ , is calculated by the equation of continuity (3)

$$\bar{u} = \left(\frac{b_1}{b_2}\right)\bar{u}_{in}, \tag{3}$$

where  $b_1$  is the external and  $b_2$  is the internal cross section length between the guide vanes. By substituting  $\bar{u}_{in}$  from Equation (2) in the above equation, the following equation emerges:

$$\bar{u} = \left(\frac{b_1}{b_2}\right)u_{\infty} \sin \frac{(2\nu - 1)\pi}{10}, \tag{4}$$

for  $\nu = 1, 2, 3, 4, 5$ . Moreover, each blade has a circumferential velocity,  $T$ ,

$$T = \Omega R, \tag{5}$$

which is in the  $x$ -axis

$$(\Omega R)_x = \Omega R \cos \alpha, \tag{6}$$

and in the  $y$ -axis, namely the axis of wind direction,

$$(\Omega R)_y = \Omega R \sin \alpha \tag{7}$$

In the above equations  $\Omega$  is the rotational velocity of the rotor,  $R$  is the rotor's radius and  $\alpha$  is the angle of attack. The resultant velocity is in the  $x$ -axis

$$u_x = (\Omega R)_x = \Omega R \cos \alpha, \tag{8}$$

and in the  $y$ -axis

$$u_y = \bar{u} \pm (\Omega R)_y = \bar{u} \pm \Omega R \sin \alpha, \tag{9}$$

where for the sections denoted by A the quantity  $\Omega R \sin \alpha$  is positive while for the sections denoted by B is negative. The resultant velocity is given by Equation (10)

$$u_{res} = \sqrt{u_x^2 + u_y^2} \tag{10}$$

By substituting in the above equation  $u_x$  and  $u_y$  from Equations (8) and (9) respectively, we get:

$$u_{res} = \sqrt{(\Omega R)_x^2 + (\bar{u} \pm \Omega R \sin \alpha)^2} \Rightarrow \tag{11}$$

$$u_{res} = \sqrt{(\Omega R)^2 \cos^2 \alpha + \bar{u}^2 + (\Omega R)^2 \sin^2 \alpha \pm 2\Omega R \sin \alpha \bar{u}} \Rightarrow \tag{12}$$

$$u_{res} = \sqrt{(\Omega R)^2 (\sin^2 \alpha + \cos^2 \alpha) \pm 2\Omega R \sin \alpha \bar{u} + \bar{u}^2} \Rightarrow \tag{13}$$

$$u_{res} = \sqrt{(\Omega R)^2 \pm 2\Omega R \sin \alpha \bar{u} + \bar{u}^2} \tag{14}$$

The resultant velocity is given by the Equation (15), by substituting  $\bar{u}$  from Equation (4) in Equation (14):

$$u_{res} = \sqrt{(\Omega R)^2 \pm 2\Omega R \sin \alpha (b_1/b_2)u_{\infty} \sin \frac{(2\nu - 1)\pi}{10} + (b_1/b_2)^2 u_{\infty}^2 \sin^2 \frac{(2\nu - 1)\pi}{10}}, \tag{15}$$

where for the sections denoted by A the quantity  $2\Omega R \sin \alpha (b_1/b_2) u_\infty \sin \frac{(2\nu-1)\pi}{10}$  is positive while for the sections denoted by B is negative. In the above equation  $\Omega$  is the rotational velocity of the rotor,  $R$  is the rotor's radius,  $\alpha$  is the angle of attack,  $b_1$  is the external and  $b_2$  is the internal cross section length between the guide vanes,  $u_\infty$  is the wind speed and  $\nu$  is the number of each section, i.e., 1, 2, 3, 4 or 5.

Then, the aerodynamic forces of lift and drag that are exerted on the blades can be determined by Equations (16) and (17)

$$L = \frac{1}{2} c_l \rho_{air} u_{res}^2, \tag{16}$$

$$D = \frac{1}{2} c_d \rho_{air} u_{res}^2 A, \tag{17}$$

where  $L$  is the lift,  $D$  is the Drag,  $c_l$  and  $c_d$  are the lift and drag coefficients respectively,  $\rho_{air}$  is the density of the air and  $A$  is the blade's area.

The resultant force,  $F$ , which is exerted on the blade and can be situated at any position is calculated by Equation (18)

$$F = \frac{1}{2} \rho_{air} u_{res}^2 \sqrt{c_d^2 + c_l^2}, \tag{18}$$

Then the aerodynamic torque can be estimated by Equation (19):

$$I = \frac{1}{2} \rho_{air} u_{res}^2 \sqrt{c_d^2 + c_l^2} R, \tag{19}$$

And finally the power output of each blade at each position is given by Equation (20):

$$P = \frac{1}{2} \rho_{air} u_{res}^2 \sqrt{c_d^2 + c_l^2} \Omega R \tag{20}$$

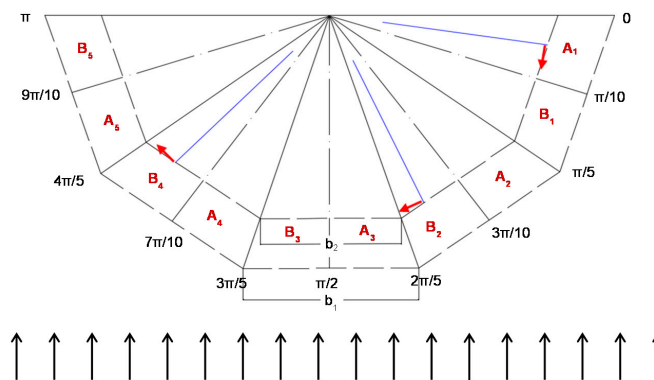


**Figure 2.** Analysis of the half top view of the stator, in order to calculate the magnitude of velocity inlet and the resultant velocity at various stator sections.

The above equations are solved by the imperative programming language FORTRAN (FORmulae TRANslator), which was originally developed for scientific and engineering applications. The resulting relationships have enabled easy parametric sizing, and so the investigation of the performance of KIONAS on the dimensions of both blades and guide vanes was conducted. Mathematical study is necessary in order to calculate the multi-stage KIONAS power output in less computational time and with less required computational memory compared to the Computational Fluid Dynamics study.

### 2.2. Computational Fluid Dynamics Study

The commercial Computational Fluid Dynamics code ANSYS Fluent [17] was used in order to show the flow field around the vertical axis wind turbine KIONAS. The first step in the simulation process is the design of the geometries of the various configurations of KIONAS in DesignModeler.

A C-type mesh was constructed; in particular KIONAS is surrounded by a semicircle and a horizontal parallelepiped. The semicircle consists of five parts defined as velocity inlets, with different velocity magnitudes depending on the relative position of the area between stator vanes and the maximum wind speed location. The rotor and the stator are defined as wall boundary conditions, the rear side as a pressure outlet and the remaining sides as symmetry.

First of all, simulations of the flow over the simplest geometry—that is, KIONAS with one stage—were conducted, in which the stator guide vanes are flat. The rotor blades are also flat plates and their inclination is  $25^\circ$  and  $45^\circ$ . After that, simulations were performed for the one-stage KIONAS, with the difference that the stator guide vanes are curved.

Finally, simulations of the flow were performed over the two-stage wind turbine KIONAS with curved stator guide vanes. This type of stator guide vane was found to be more effective and for that reason it was selected for the simulations. The rotor blades inclination was  $25^\circ$ ,  $30^\circ$  and  $35^\circ$ . Figure 3 shows the rotor, the stator and the computational domain over the two-stage KIONAS.

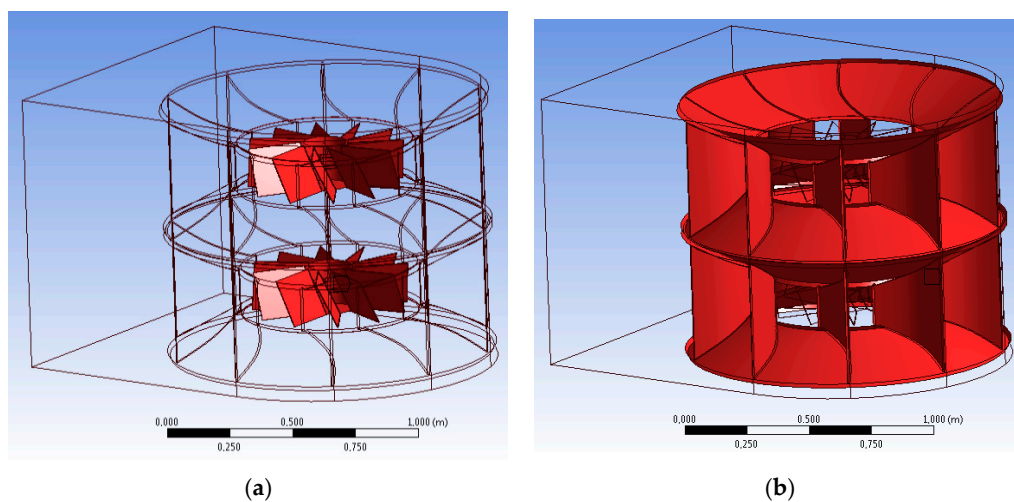


**Figure 3.** (a) Rotor; (b) stator of two-stage wind turbine KIONAS and computational domain.

The grid independence study revealed that a mesh of 1,412,500 cells for the one-stage KIONAS and of 2,825,000 cells for the two-stage KIONAS would be sufficient to establish a grid-independent solution. The mesh was denser near the wind turbine, where changes in the flow occur and thus greater computational accuracy is necessary.

The rotation was simulated by the Moving Reference Frame Model (MRF) [18], a steady-state approximation in which individual cell zones move at different rotational and/or translational speeds, and the most appropriate turbulence model for such simulations is the  $k-\omega$  shear-stress transport (SST) [19]. In the MRF model, the rotor of KIONAS and the domain surrounding it were defined as a rotating reference frame, while the stator of KIONAS, in other words the flow outside the rotor region, was defined as a stationary frame.

### 3. Results and Discussion

#### 3.1. Mathematical Results

This section summarizes the results obtained from the mathematical study. Figure 4 presents the total power at each blade's position for wind speeds of 5 m/s and 10 m/s and rotors with various numbers of blades. The results indicate that adding more blades results in higher values of total power for the wind speed that were tested. The results obtained from the analysis of rotors with 2 to 11 blades are summarized in Table 1. The results indicate that there is a significant positive correlation between the numbers of blades and the mean power output of KIONAS. Although most wind turbines achieve

an optimized performance with a rotor which consists of three blades, there are plenty smaller scale turbines or at higher speeds, the efficiency of which increases by adding more blades. KIONAS is such a configuration of a vertical axis wind turbine, because not only it is a small scale wind turbine but also its rotor experiences high speeds as the wind velocity is accelerated when it passes through the stator that surrounds the rotor.

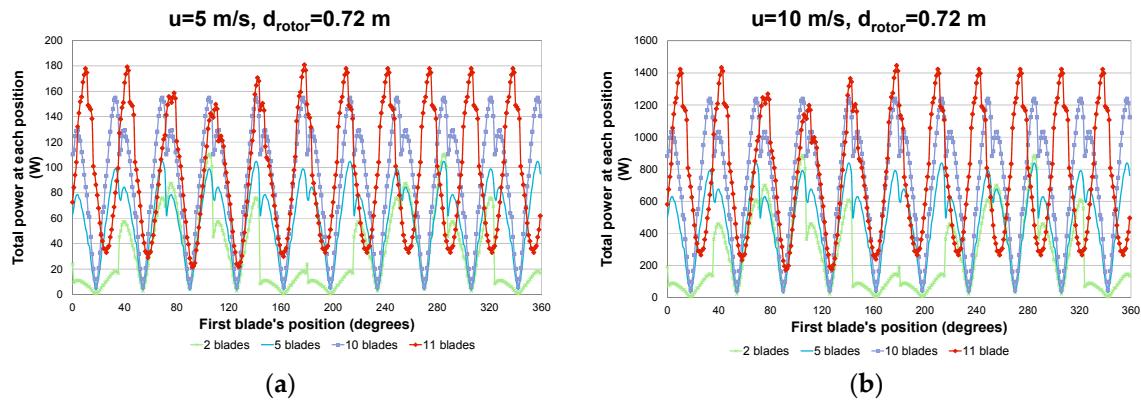


**Figure 4.** Total power at each blade’s position for wind velocity (a) 5 m/s; (b) 10 m/s for various numbers of blades.

**Table 1.** Mean power output in Watts for wind speed of 5 m/s and 10 m/s for various numbers of blades.

	Wind Speed $u = 5 \text{ m/s}$	Wind Speed $u = 10 \text{ m/s}$
2 blades	32.9	263.6
3 blades	42.1	336.7
4 blades	50.3	402.1
5 blades	57.8	462.2
6 blades	64.8	440.3
7 blades	71.4	571.5
8 blades	77.8	622.1
9 blades	83.8	670.7
10 blades	89.7	717.6
11 blades	95.4	762.8

An estimation of the power output between KIONAS with blades made of galvanized sheet metal and KIONAS with blades made of aluminum is presented in Figure 5. The greater density of galvanized sheet metal, which means greater weight of the blades, results in lower rotational speed of the rotor and thus less power output.

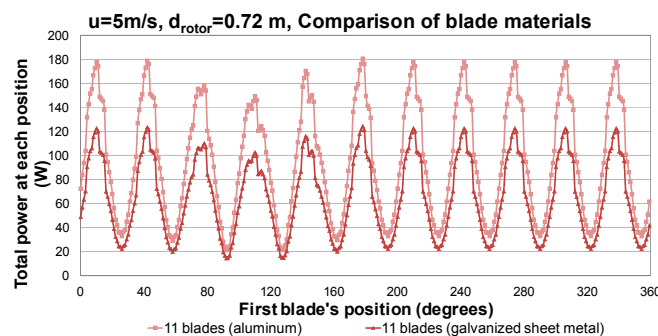


**Figure 5.** Total power at each blade’s position, for eleven rotor blades made of aluminum or galvanized sheet metal.

Figure 6 demonstrates the total power at each blade’s position for the same wind speeds and different rotor diameters. The rotor diameter is the diameter that occurs when the stator’s diameter increases by 150% and 200%, while its width remains constant. From this data it is obvious that the power of KIONAS increases when increasing the rotor’s number of blades and diameter.

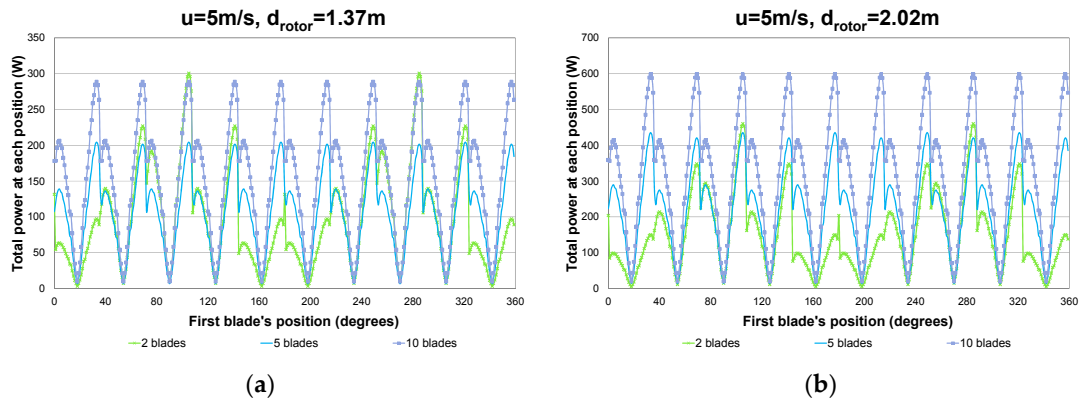


Figure 6. Total power at each blade’s position for wind velocity 5 m/s, various numbers of blades and rotor’s diameter (a) 1.37 m; (b) 2.02 m.

Table 2 compares the mean power output in Watts for wind speed equal to 5 m/s and the initial rotor diameter of 0.72 m and the new rotor diameters of 1.37 m and 2.02 m. It can be seen from the data that the mean power output of the wind turbine increases as the rotor diameter and number of blades increase.

Table 2. Mean power output in Watts for various rotor diameters and various numbers of blades.

	$d_{rotor} = 0.72 \text{ m}$	$d_{rotor} = 1.37 \text{ m}$	$d_{rotor} = 2.02 \text{ m}$
2 blades	32.9	55.5	81.1
5 blades	57.8	93.5	132.4
10 blades	89.7	141.9	198.3

Figure 7 shows the total power at each blade’s position for eleven blades with and without inclination, rotor blade angle of 25 degrees and wind velocity 5 m/s and 10 m/s. It is obvious that the power output is reduced by the inclination of the blades, because it was assumed that the inclined blade has greater length and thus greater weight, and that leads to lower rotational speed.

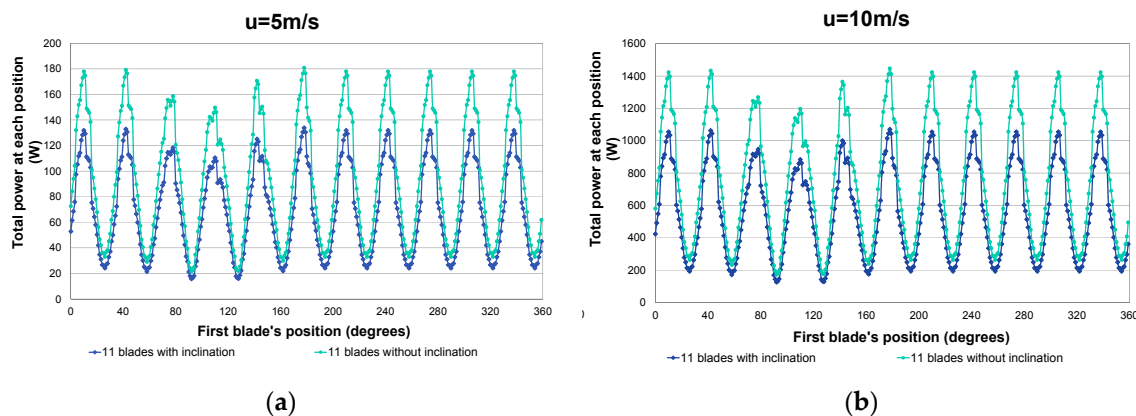


Figure 7. Total power at each blade’s position for eleven rotor blades with 25° inclination and without inclination and wind velocity (a) 5 m/s; (b) 10 m/s.

To determine the effects of adding more stages, the total power of different KIONAS types is compared and the results are presented in Figure 8. The results are referred in wind velocity of 5 m/s and diameter of the rotor equal to 0.72 m. There was a significant positive correlation between total power and number of KIONAS stages. Further statistical tests revealed the exact percentage contribution of each stage in the total power of different KIONAS types and Figure 9 shows these results.

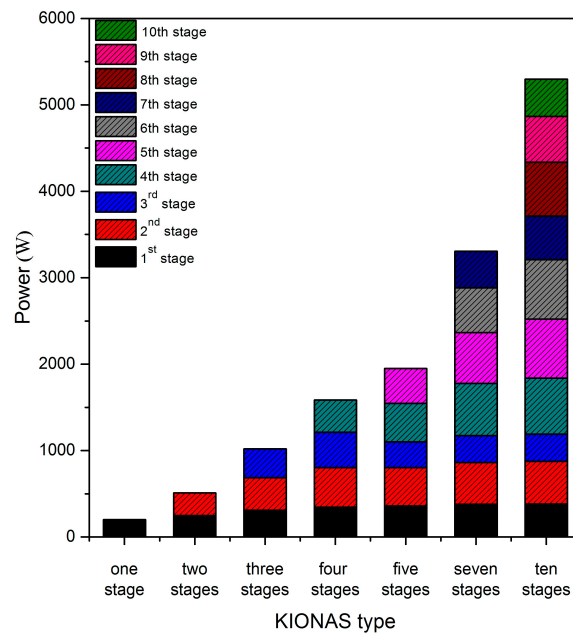


Figure 8. Total power output in Watts for various KIONAS types.

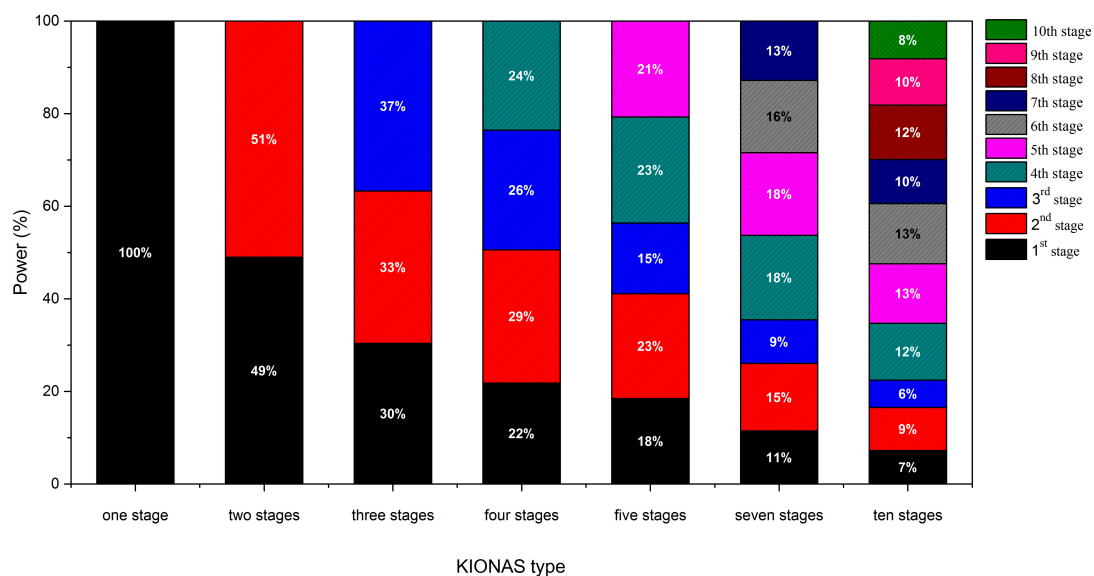


Figure 9. Each stage’s contribution in the total power of each KIONAS type.

The percentage increase in power of each stage when it is placed in KIONAS, which has an extra stage, was also investigated and is presented in Figure 10. The most striking result to emerge from the data is that, for example, when the first stage is alone, it has a power of 200.1 W, but when it is placed in a two-stage KIONAS, the first stage power is 249.4 W; in other words, it increases 24.6%. Interestingly, if the first stage is placed in a ten-stage KIONAS, its increase is 91.4%.

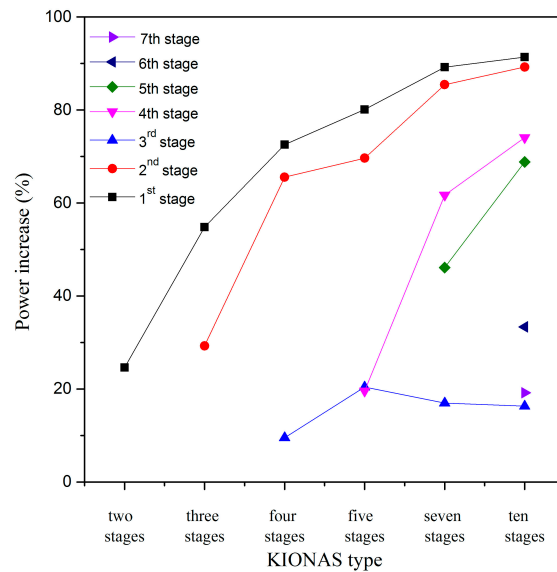


Figure 10. Each stage’s increase in power by adding additional stages.

Figure 11 provides the power coefficient versus KIONAS weight and the power per weight unit for various KIONAS types. There is a clear trend of the power coefficient decreasing with KIONAS weight, due to the fact that the power coefficient is inversely proportional to the swept area, which increases by adding more stages because the surface between the stages is included too. Of particular interest is the correlation between power per KIONAS weight and KIONAS type, because despite the increase in the weight of the machine, which means an increase in the cost of construction, the power output is much higher, so a multi-stage KIONAS could become advantageous in the long term.

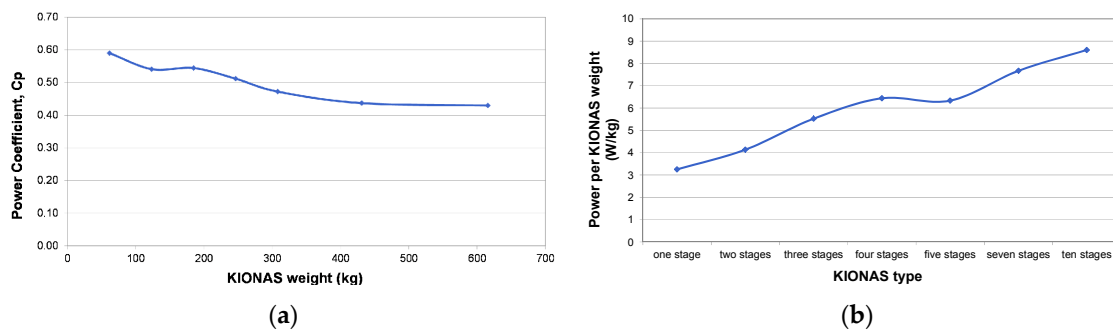
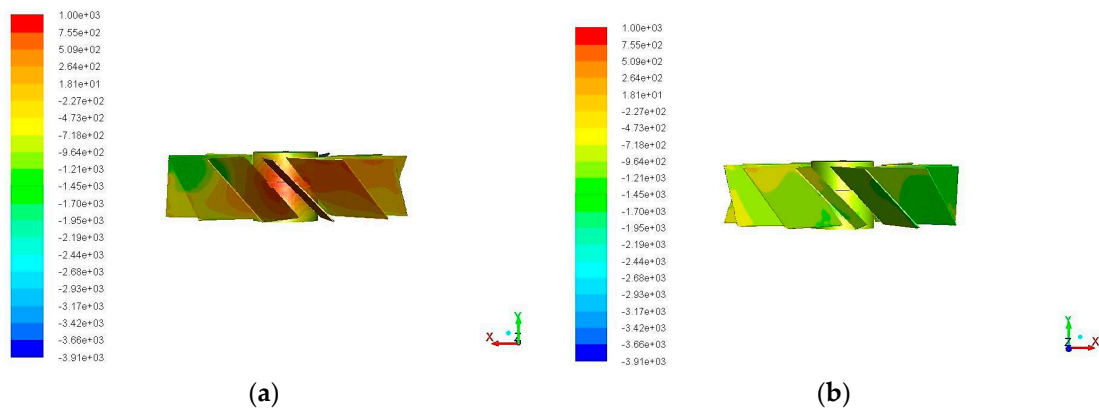


Figure 11. (a) Power coefficient vs KIONAS weight; (b) Power per weight for various KIONAS types.

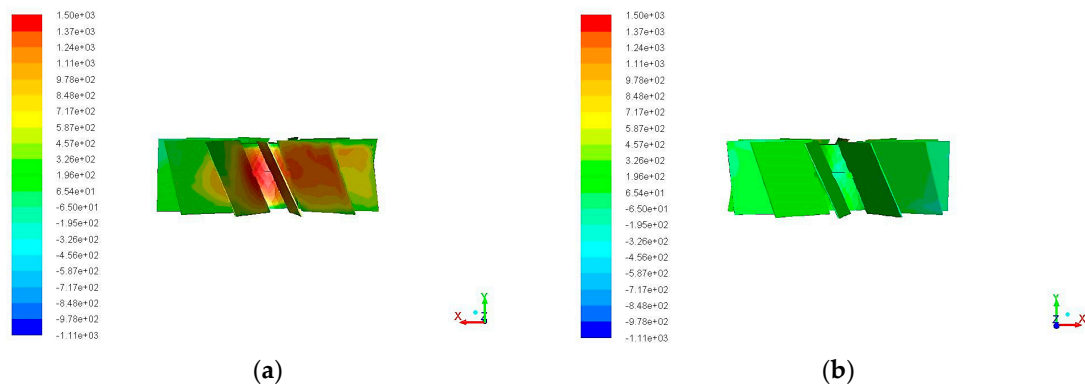
### 3.2. Computational Fluid Dynamics Results

In this section, the results obtained from the Computational Fluid Dynamics are summarized. In Figures 12 and 13 the static pressure distribution on the rotor with rotor blades angles of 45° and 25°, respectively, and flat stator guide vanes, which was calculated by ANSYS Fluent, is presented. It is obvious that the contested surface of the rotor has higher values of static pressure and the rotor rotates due to this pressure difference. The values of static pressure on the rotor blades with inclination of 25° are higher than the corresponding values of inclination of 45°.

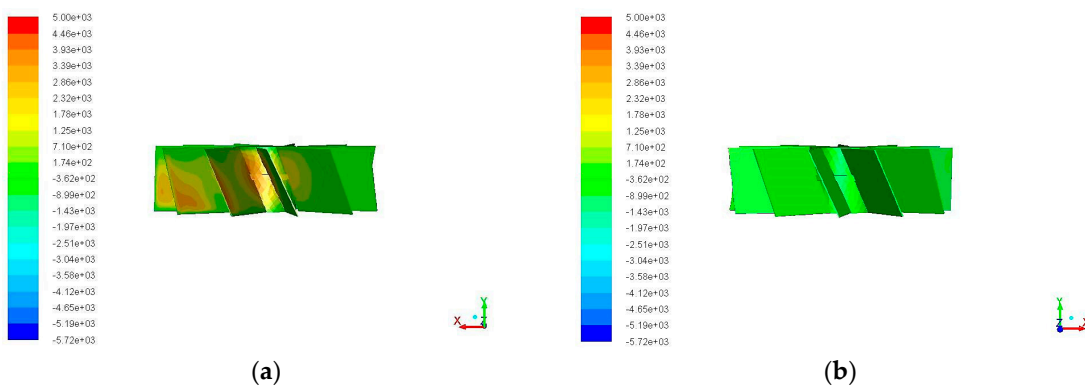
Simulation of the flow over a one-stage KIONAS with rotor blade angle of 25° and stator with curved guide vanes was also conducted and the results of the static pressure distribution on the rotor are presented in Figure 14. From the comparison between Figures 13 and 14, it is concluded that in the case of curved stator vanes, the static pressure is greater.



**Figure 12.** Static pressure (Pa) distribution (a) on the contested surface; (b) on the non-contested surface of a one-stage KIONAS, rotor blade angle of 45 degrees and stator with flat guide vanes.

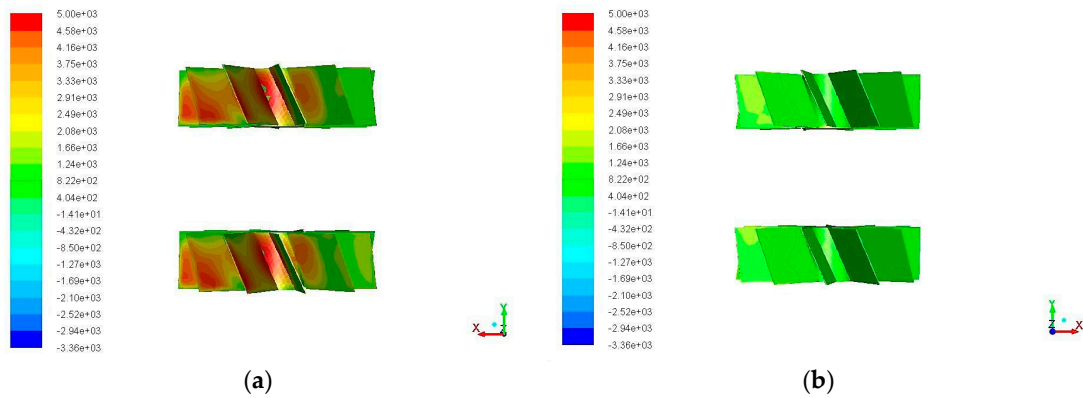


**Figure 13.** Static pressure (Pa) distribution (a) on the contested surface; (b) on the non-contested surface of one-stage KIONAS, rotor blade angle of 25 degrees and stator with flat guide vanes.



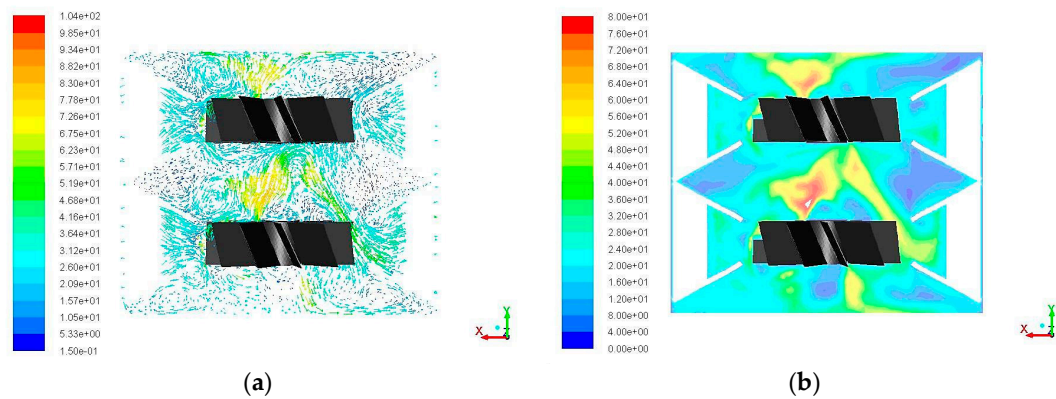
**Figure 14.** Static pressure (Pa) distribution (a) on the contested surface; (b) on the non-contested surface of one-stage KIONAS, rotor blade angle of 25 degrees and stator with curved guide vanes.

Figure 15 shows the static pressure distribution on the rotor with a rotor blade angle of 25° and stator with curved guide vanes of two-stage KIONAS. The static pressure is greater on the contested surface of the rotors and on the upper rotor. This result implies that the rotational velocity of the rotor which is located on the upper stage is greater, and thus the power of the upper stage is greater as well. This finding is consistent with Figure 9, where the power of the second stage of a two-stage KIONAS is greater than the power of the first stage.



**Figure 15.** Static pressure (Pa) distribution (a) on the contested surface; (b) on the non-contested surface of two-stage KIONAS, rotor blade angle of  $25^\circ$  and stator with curved guide vanes.

From Figures 16–18 the velocity vectors and the contours of velocity for two-stage KIONAS, stator with curved guide vanes and rotor blade angle of  $25^\circ$ ,  $30^\circ$  and  $35^\circ$  are illustrated. The most interesting finding from these Figures is that part of the wind is directed towards the top and towards the lower stage for all the cases that examined, and this move of air mass into KIONAS structure affects the power of each stage when it is placed in KIONAS with an extra stage.



**Figure 16.** (a) Velocity vectors (m/s); (b) contours of velocity (m/s) on  $xy$  plane and the center of the rotor for two-stage KIONAS, rotor blade angle of  $25^\circ$  and stator with curved guide vanes.

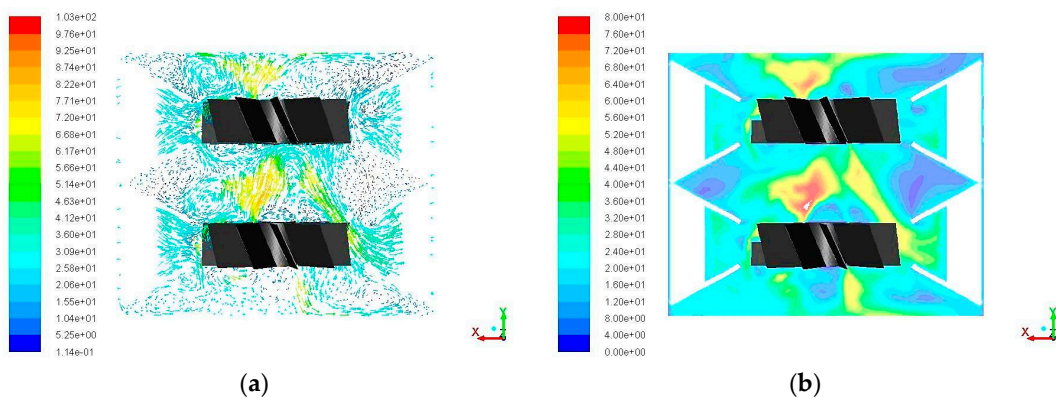


**Figure 17.** (a) Velocity vectors (m/s); (b) contours of velocity (m/s) on  $xy$  plane and the center of the rotor for two-stage KIONAS, rotor blade angle of  $30^\circ$  and stator with curved guide vanes.

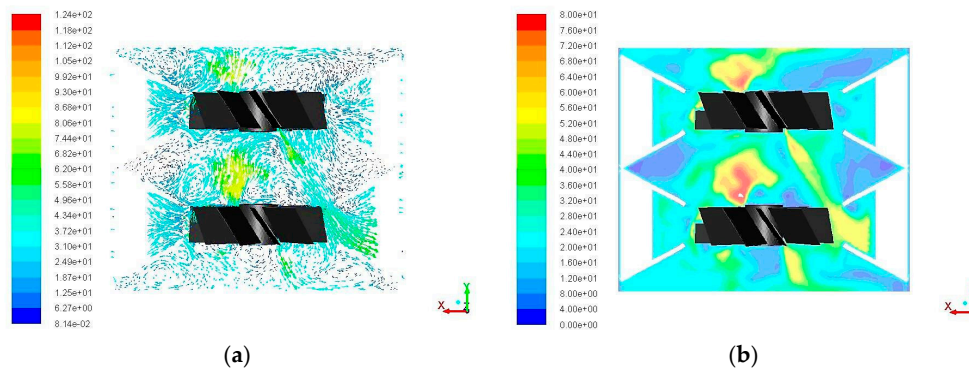


**Figure 18.** (a) Velocity vectors (m/s); (b) contours of velocity (m/s) on  $xy$  plane and the center of the rotor for two-stage KIONAS, rotor blade angle of  $35^\circ$  and stator with curved guide vanes.

#### 4. Conclusions

This project was undertaken to describe the design and evaluate the aerodynamic performance of the wind turbine KIONAS. This study/research has shown that the power output of the wind turbine increases as the diameter and the number of rotor blades increase. It was also shown that the power output for KIONAS with inclined blades is reduced, due to the increased mass of each blade when it has any inclination. Another major finding was that the curved guide vanes in the stator of KIONAS result in higher power.

The most significant findings to emerge from this study are not only that the power of each individual stage is increased when an extra stage is added but also that the output power per unit weight of the machine is higher as the number of KIONAS stages is increased. That means that a multi-stage KIONAS could become advantageous in the long term.

The results of the computational investigation show that the static pressure is greater in the contested surface of KIONAS and the pressure difference between the front and the rear side of the rotor is responsible for the rotor rotation. The velocity vectors for the two-stage KIONAS indicate that part of the wind is directed both towards the upper and towards the lower stage. Further experimental investigations would be of great help in assessing the actual attitude of KIONAS and this information would help to include more factors affecting the flow in the mathematical analysis.

The evidence from this study suggests that, in general, the present wind turbine cannot compete with the large structures that produce power in the range of 1, 2 and 3 MW, but is a major competitor with the smallest structures of the 5, 10 and 100 kW range. This power may vary with larger diameter dimensions, lighter material, but also with higher wind speeds, in order to cover the needs of individual houses or small settlements. A great benefit of KIONAS is the simple construction of both the guide vanes and the rotor blades, along with its compact shape which can easily be mounted in spaces of small dimensions either on buildings or between them, without creating problems in terms of adaptability in space or public acceptance.

**Acknowledgments:** This work was part of the project Evaluation and Optimization of Innovation of a Vertical Axis Wind Turbine (ABAKA) and was supported by BIG SOLAR S.A. member of the BITROS Group of Companies.

**Author Contributions:** Eleni Douvi conducted the simulations for the computational fluid dynamics study and wrote the paper; Dimitra Douvi carried out the mathematical study; Eleni Douvi, Dimitra Douvi and Dionissios Margaris analyzed the data; Ioannis Drosis invented the KIONAS vertical axis wind turbine.

**Conflicts of Interest:** The authors declare no conflict of interest.

#### References

1. Aslam Bhutta, M.M.; Hayat, N.; Farooq, A.U.; Ali, Z.; Jamil, S.R.; Hussain, Z. Vertical axis wind turbine—A review of various configurations and design techniques. *J. Renew. Substain. Energy Rev.* **2012**, *16*, 1926–1939. [[CrossRef](#)]

2. Tang, Z.; Yao, Y.; Zhou, L.; Yu, B. A review on the new structure of savonius wind turbines. *J. Adv. Mater. Res.* **2013**, *608–609*, 467–478. [[CrossRef](#)]
3. Ejiri, E.; Yabe, S.; Hase, S.; Ogiwara, M. Unsteady flow analysis of the vertical axis cross-flow wind turbine. In Proceedings of the ASME Fluids Engineering Division Summer Conference, Miami, FL, USA, 17–20 July 2006.
4. Takao, M.; Maeda, T.; Kamada, Y.; Oki, M.; Kuma, H. A straight-bladed vertical axis wind turbine with a directed guide vane row. In Proceedings of the 5th Joint ASME/JSME Fluids Engineering Summer Conference, San Diego, CA, USA, 30 July–8 August 2007.
5. Takao, M.; Takita, H.; Saito, Y.; Maeda, T.; Kamada, Y.; Toshimitsu, K. Experimental study of a straight-bladed vertical axis wind turbine with a directed guide vane row. In Proceedings of the 28th International Conference on Offshore Mechanics and Arctic Engineering—OMAE, Honolulu, HI, USA, 31 May–5 June 2009.
6. Shahizare, B.; Nik Ghazali, N.N.B.; Chong, W.T.; Tabatabaieikia, S.S.; Izadyar, N. Investigation of the optimal omni-direction-guide-vane design for vertical axis wind turbines based on unsteady flow CFD simulation. *J. Energies* **2016**, *9*, 1–25. [[CrossRef](#)]
7. Kim, D.; Gharib, M. Efficiency improvement of straight-bladed vertical-axis wind turbines with an upstream deflector. *J. Wind Eng. Ind. Aerodyn.* **2013**, *115*, 48–52. [[CrossRef](#)]
8. Korprasertsak, N.; Leephakpreeda, T. Analysis and Optimal Design of Wind Boosters for Vertical Axis Wind Turbines at Low Wind Speed. *J. Wind Eng. Ind. Aerodyn.* **2016**, *159*, 9–18. [[CrossRef](#)]
9. Wong, K.H.; Chong, W.T.; Yap, H.T.; Fazlizan, A.; Omar, W.Z.W.; Poh, S.C.; Hsiao, F.B. The design and flow simulation of a power-augmented shroud for urban wind turbine system. *J. Energy Procedia* **2014**, *61*, 1275–1278. [[CrossRef](#)]
10. Nobile, R.; Vahdati, M.; Barlow, J.F.; Mewburn-Crook, A. Unsteady flow simulation of a vertical axis augmented wind turbine: A two-dimensional study. *J. Wind Eng. Ind. Aerodyn.* **2014**, *125*, 168–179. [[CrossRef](#)]
11. Chen, T.Y.; Liao, Y.T.; Chen, Y.Y.; Liou, J.L. Application of a vortical stator assembly to augment the rotor performance of drag-type vertical-axis wind turbines. *J. Aeronaut. Astronaut. Aviat. Ser. A* **2015**, *47*, 75–84.
12. Chen, T.Y.; Chen, Y.Y. Developing a Vortical Stator Assembly to Improve the Performance of Drag-Type Vertical-Axis Wind Turbines. *J. Mech.* **2015**, *31*, 693–699. [[CrossRef](#)]
13. Pope, K.; Rodrigues, V.; Doyle, R.; Tsopelas, A.; Gravelsins, R.; Naterer, G.F.; Tsang, E. Effects of stator vanes on power coefficients of a zephyr vertical axis wind turbine. *J. Renew. Energy* **2010**, *35*, 1043–1051. [[CrossRef](#)]
14. Burlando, M.; Ricci, A.; Freda, A.; Repetto, M.P. Numerical and experimental methods to investigate the behaviour of vertical-axis wind turbines with stators. *J. Wind Eng. Ind. Aerodyn.* **2015**, *144*, 125–133. [[CrossRef](#)]
15. Chong, W.T.; Muzammil, W.K.; Fazlizan, A.; Hassan, M.R.; Taheri, H.; Gwani, M.; Kothari, H.; Poh, S.C. Urban Eco-Greenergy™ hybrid wind-solar photovoltaic energy system and its applications. *J. Precis. Eng.* **2015**, *16*, 1263–1268. [[CrossRef](#)]
16. Tong, C.W.; Zainon, M.Z.; Chew, P.S.; Kui, S.C.; Keong, W.S.; Chen, P.K. Innovative power-augmentation-guide-vane design of wind-solar hybrid renewable energy harvester for urban high rise application. In Proceedings of the 10th Asian International Conference on Fluid Machinery, Kuala Lumpur, Malaysia, 21–23 October 2010; pp. 507–521.
17. ANSYS® Academic Research, Release 16.0. Available online: <http://www.ansys.com/> (accessed on 10 January 2017).
18. Luo, J.Y.; Issa, R.I.; Gosman, A.D. Prediction of Impeller-Induced Flows in Mixing Vessels Using Multiple Frames of Reference. In *IChemE Symposium Series*; The Institution of Chemical Engineers: Rugby, UK, 1994; pp. 549–556.
19. Menter, F.R. Two-Equation Eddy-Viscosity Turbulence Models for Engineering Applications. *AIAA J.* **1994**, *32*, 1598–1605. [[CrossRef](#)]

